



Bioprocess development for muconic acid production from aromatic compounds and lignin

Journal:	<i>Green Chemistry</i>
Manuscript ID	GC-ART-08-2018-002519.R2
Article Type:	Paper
Date Submitted by the Author:	05-Oct-2018
Complete List of Authors:	Salvachua, Davinia; National Renewable Energy Laboratory, National Bioenergy Center Johnson, Christopher; National Renewable Energy Laboratory, National Bioenergy Center Singer, Christine; National Renewable Energy Laboratory, National Bioenergy Center Rohrer, Holly; National Renewable Energy Laboratory, National Bioenergy Center Peterson, Darren; National Renewable Energy Laboratory, National Bioenergy Center Black, Brenna; National Renewable Energy Laboratory, National Bioenergy Center Knapp, Anna; National Renewable Energy Laboratory, National Bioenergy Center Beckham, Gregg; National Renewable Energy Laboratory, National Bioenergy Center





Green Chemistry

PAPER

View Article Online
View Journal | View Issue

Process development for muconic acid production from aromatic compounds and lignin†

Davinia Salvachúa*, Christopher W. Johnson, Christine A. Singer, Holly Rohrer, Darren J. Peterson, Brenna A. Black, Anna Knapp, Gregg T. Beckham*

Muconic acid (MA) is a bio-based platform chemical that can be converted into the commodity petrochemical building blocks adipic acid or terephthalic acid, or used in emerging, performance-advantaged materials. MA is a metabolic intermediate in the β -ketoacid pathway, and can be produced from carbohydrates or other traditional carbon sources via the shikimate pathway. MA can also be produced from lignin-derived aromatic compounds with high atom efficiency through aromatic-catabolic pathways. Metabolic engineering efforts to date have developed efficient muconic acid-producing strains of the aromatic-catabolic microbe *Pseudomonas putida* KT2440, but the titers, productivities, and yields from aromatic compounds in most cases remain below the thresholds needed for industrially-relevant bioreactor cultivations. To that end, this work presents further process and host development towards improving MA titers, yields, and productivities, using the hydroxycinnamic acids, *p*-coumaric acid and ferulic acid, as model aromatic compounds. Coupling strain engineering and bioprocess development enabled the discovery of new bottlenecks in *P. putida* that hinder MA production from these compounds. A combination of gene overexpression and removal of a global catabolic regulator resulted in high-yielding strains (100% molar yield). Maximum MA titers of 50 g/L, which is near the lethal toxicity limit in this bacterium, and productivities over 0.5 g/L/h were achieved in separate process configurations. Additionally, a high-pH feeding strategy, which could potentially reduce the salt load and enable higher titers by decreasing product dilution, was tested with model compounds and lignin-rich streams from corn stover and a complete conversion of the primary monomeric aromatic compounds to MA was demonstrated, obtaining a titer of 4 g/L. Overall, this study presents a step forward for the production of value-added chemicals from lignin and highlights critical needs for further strain improvement and bioprocess development that can be applied in the biological valorization of lignin.

Address: National Bioenergy Center, National Renewable Energy Laboratory, Golden, CO, United States

* gregg.beckham@nrel.gov; davinia.salvachua@nrel.gov

Keywords: *Pseudomonas putida* KT2440 | Fermentation | Bioreactor | Lignin valorization | Aromatic catabolism

† Electronic supplementary information (ESI) available.

Introduction

Muconic acid (MA) is an unsaturated, C6-dicarboxylic acid that can be readily converted into the commercial commodity chemicals adipic acid¹⁻³ and terephthalic acid.⁴ MA can also be partially hydrogenated to 3-hexenedioic acid, which can be used in the production of improved nylons,^{5,6} or used directly for the production of performance-advantaged composites.^{7,8} Given its versatility in the production of direct replacement chemicals and in performance-advantaged bioproducts, MA has recently been highlighted as a “bioprivileged” molecule by Shanks and Keeling.⁹ The seminal work in the peer-reviewed literature of biological MA production was reported by Draths and Frost,² who developed an engineered *Escherichia coli* strain capable of producing MA from glucose via shikimate pathway at a molar yield of 30%. Further efforts to produce MA from glucose have focused on evaluating different hosts, such as *Saccharomyces cerevisiae*,^{10, 11} and increasing MA titers by employing different engineered *E. coli*¹² or *Pseudomonas putida* KT2440¹³ strains. Apart from glucose, MA can be also produced from aromatic compounds via β -ketoacid pathway,³ at a theoretical yield and an atom efficiency much higher than from glucose, making the aromatic heteropolymer, lignin, an attractive and renewably-sourced feedstock for MA production.

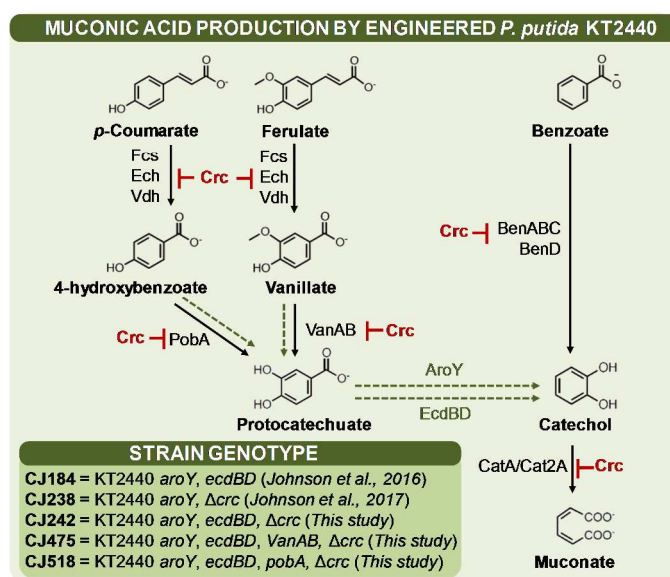


Fig. 1 Overview of metabolic pathways and genotype differences of the MA-producing strains utilized in the current work. The complete genotype is presented in **Table S1**. Continuous arrows represent native pathways in *P. putida* KT2440, discontinuous arrows indicate genetic insertions or overexpressions, and red markers highlight putative targets for *Crc* regulation.

Lignin, the most recalcitrant polymer in lignocellulose, is highly undervalued, and its upgrading is recognized as critical to support the feasibility of modern lignocellulosic biorefineries.¹⁴⁻¹⁶ In this regard, a recent techno-economic analysis revealed that fuel prices from cellulosic sugars could be reduced by up to \$3 per gasoline-gallon equivalent if the lignin from the biorefinery was converted in an 80% yield to MA and catalytically upgraded to adipic acid.¹⁶ Furthermore, the biorefinery sustainability when converting lignin to MA and adipic acid remains environmentally beneficial even when lignin is diverted away from heat and power,¹⁷ which has been the main route for lignin to date. Currently, lignin depolymerization is one of the main challenges if monomeric species are needed for further valorization. However, many chemical and biological strategies exist and are being actively developed for this purpose.^{14, 15, 18-20}

The most well studied aromatic precursor for MA production has been benzoic acid,³ but this compound is not a typical monomer released during lignin depolymerization. Consequently, with the aim of valorizing lignin, the substrate spectrum for the production of MA has broadened in the last years and new model compounds and diverse lignin streams have been tested (Table 1). However, MA titers and yields from lignin streams typically remain low. In terms of host selection, due to its robustness, tolerance to aromatic compounds, and the presence of endogenous aromatic-catabolic pathways (β -ketoacid pathway) (Fig. 1), *P. putida* KT2440 has been the primary bacterial strain engineered for MA production. Engineered *E. coli*, *Corynebacterium glutamicum*, and *Arthrobacter* sp. have also been reported to produce high MA titers from aromatic compounds such as catechol and benzoic acid (Table 1).

In addition to producing high yields of bioavailable compounds from lignin depolymerization, it is also necessary to simultaneously work to improve the strains and associated bioprocesses to move towards industrially-relevant titers, productivities, and yields. In this regard, little work has been directed to optimize MA production processes utilizing lignin-relevant aromatic compounds (i.e. hydroxycinnamic acids released from alkaline biomass treatments methods such as *p*-coumaric acid (*p*-CA) and ferulic acid (FA)),^{4, 21} which is critical to identify strain and process limitations. Recently, we have demonstrated improvements in *P. putida* KT2440 strains (hereafter KT2440) in terms of MA yields from *p*-CA by (1) enhancing the activity of the protocatechuate decarboxylase (AroY) through the co-expression of two associated proteins (EcdBD) (generating the strain KT2440-CJ184)^{13, 22} and by (2) eliminating a global regulator of carbon catabolite repression (generating the strain KT2440-CJ238)²³ (Fig. 1). However, our previous work did not focus on increasing MA titer or productivity – key cost drivers for any bioprocess.

The aim of this work is to evaluate new and previously reported KT2440 strains in various bioreactor setups to identify bottlenecks and further develop an efficient MA production process and strain. For that purpose, we used monomeric aromatic compounds, namely *p*-CA and FA, as model substrates and evaluated the effect of different feeding strategies to achieve high MA titer, yield, and productivity. In addition, we also evaluated MA production from two high pH lignin-rich streams produced in a biorefinery-like process from corn stover.²⁴ Overall this work provides new insights regarding both substrate and product toxicity and highlights additional bottlenecks for further strain and process improvements that could be applied to a variety of lignin streams.

Table 1 Comparative muconic acid (MA) titers reported from aromatic compounds and lignin streams. Yield is calculated as MA mol per mol of aromatic compound (model or detected in the lignin stream). Productivity is calculated as MA titer at the end time point divided by the total cultivation time. APL=alkaline pretreated liquor; BCDL=lignin liquor resulting from base catalyzed depolymerization; DO=Oxygen saturation; FB=fed-batch.

Microorganism	Substrate	Feeding mode	Titer g/L	Yield mol/mol	Productivity g/L/h	Reference
AROMATIC COMPOUNDS						
<i>E. coli</i> BL21 (DE3)/pEcatA	Catechol	FB	59.0	1.00	4.90	25
<i>P. putida</i> KT2440-MA1	Catechol	pH-stat FB	64.2	1.00	1.03	26
<i>C. glutamicum</i> MA-2	Catechol	DO-stat FB	85.0	1.00	1.42	27
<i>P. putida</i> BM014	Benzoate	Constant FB, cell-recycle	13.5	1.00	5.50	28
<i>P. putida</i> KT2440-JD1	Benzoate	pH-stat FB	18.5	1.00	0.80	29
<i>P. putida</i> BM014	Benzoate	DO-stat FB	32.4	1.00	0.70	30
<i>P. putida</i> KT2440-CJ102	Benzoate	DO-stat FB	34.5	1.00	0.28	31
<i>Arthrobacter</i> sp. T8626	Benzoate	Manual FB	44.1	0.96	0.90	32
<i>P. putida</i> KT2440-CJ242	Benzoate	DO-stat FB	52.3	0.97	0.26	This work
<i>P. putida</i> KT2440-CJ184	<i>p</i> -Coumarate	DO-stat FB	15.6	1.00	0.21	13
<i>P. putida</i> KT2440-CJ242	<i>p</i> -Coumarate	DO-stat FB	29.4	0.98	0.20	This work
<i>P. putida</i> KT2440-CJ242	<i>p</i> -Coumarate	Constant FB	27.1	0.99	0.53	This work
<i>P. putida</i> KT2440-CJ242	<i>p</i> -Coumarate	Constant FB, high pH feed	49.7 ^a /27.7 ^b	0.97 ^a /0.99 ^b	0.23 ^a /0.49 ^b	This work
<i>P. putida</i> KT2440-CJ475	Ferulate	Constant FB	16.0	0.99	0.21	This work
<i>P. putida</i> KT2440-CJ475	<i>p</i> -Coumarate + Ferulate	Constant FB	34.7 ^c /27.1 ^d	1.00 ^c /0.99 ^d	0.27 ^c /0.50 ^d	This work
LIGNIN STREAMS						
<i>P. putida</i> KT2440 IDPC/pTS108	Japanese cedar	FB	0.02	0.001	0.001	33
<i>Sphingobium</i> sp. SYK6 SME257/pTS084	Birch	FB	0.03	0.41	0.001	33
<i>E. coli-engineered</i>	Kraft lignin	Batch	0.34	0.74	0.007	34
<i>E. coli-engineered</i>	Tobacco	Batch	0.31	0.34	0.006	34
<i>P. putida</i> KT2440-CJ103	Corn stover BCDL	FB	0.50	0.31	0.014	21
<i>P. putida</i> KT2440-CJ103	Corn stover APL	Batch	0.70	0.67	0.029	4
<i>P. putida</i> KT2440-CJ242	Corn stover APL	Constant FB, high pH feed	0.70	1.35 ^e	0.010	This work
<i>C. glutamicum</i> MA-2	Pine	FB	1.8	1.00	0.066	27
<i>P. putida</i> KT2440-CJ242	Corn stover BCDL	Constant FB, high pH feed	3.70	1.37 ^e	0.060	This work
<i>P. putida</i> KT2440-MA9	Pine (concentrated stream)	FB by pulses	13.00	1.00	0.240	26

(a) Feeding rate at 3 mmol/h; (b) Feeding rate at 6 mmol/h; (c) Feeding rate at 4 mmol/h; (d) Feeding rate at 8 mmol/h; (e) A yield higher than 1.0 can be the result of the conversion of other non-detected aromatic compounds to MA or the utilization of oligomeric lignin.

Results

MA production from *p*-CA: the feeding strategy is key to evaluate bacterial strains

p-CA is the most abundant aromatic compound resulting from alkaline treatment of corn stover^{21, 35, 36} since esterified *p*-coumaryl groups are abundant in it (up to 18% of the total lignin)³⁷ and ester bonds are cleaved by mild base treatment.²¹ Therefore, we selected *p*-CA as an initial model aromatic compound to compare the performance of engineered MA-producing KT2440 strains. Because *p*-CA leads to MA production, a carbon and energy source (glucose in this study) also needs to be supplied to maintain the bacterial metabolism. Feeding high concentrations of aromatic compounds or glucose can have deleterious effects on KT2440, via toxicity³⁸ or catabolite repression,²³ respectively, which would ultimately hinder MA production. Thus, we selected a feeding strategy based on the saturation of oxygen (DO-stat fed-batch) to maintain both compounds at low concentrations.³⁰ To select an appropriate *p*-CA:glucose molar ratio, we conducted a preliminary experiment with a previously reported MA-producing strain, KT2440-CJ184 (*aroY* and *ecdBD* overexpressed; **Fig. 1, Table S1**).¹³ The ratios utilized were 2:1, 4:1, and 8:1. The 8:1 ratio led to the accumulation of the metabolic intermediates 4-hydroxybenzoate and protocatechuate and produced low cell biomass (**Fig. S1**). The 2:1 and 4:1 ratios generated similar MA titers (~28 g/L) and yields (>0.97 mol/mol). However, the 4:1 ratio exhibits lower cell density and a higher variability between bioreactors in terms of 4-hydroxybenzoate accumulation. Thus, we selected a *p*-CA:glucose molar ratio of 2:1 to conduct further strain evaluation.

The strains compared here were the previously reported KT2440-CJ184¹³ and KT2440-CJ238 (*aroY* overexpressed

and *Crc* knocked out, respectively, **Fig. 1, Table S1**)²³ strains, and a new strain which combines the genetic modifications from KT2440-CJ184 and KT2440-CJ238 (KT2440-CJ242) (**Fig. 1, Table S1**). The modifications to these strains are integrated into the genome, obviating the need to supplement the cultures with antibiotics. As explained above, the initial strategy selected for the feeding was DO-stat fed-batch (**Fig. 2A-C**). The oxygen profiles for all these cultivations are shown in **Fig. S2**. The performance of KT2440-CJ184 and KT2440-CJ242 was similar. Both strains achieve titers of approximately 28 g/L, yields over 0.95 mol/mol, and productivities of 0.20 g/L/h. However, KT2440-CJ238 accumulated protocatechuate during the cultivation, leading to a MA yield decrease and cell death in one of the bioreactors (**Fig. 2B, Fig. S2B**).

DO-stat feeding strategies are appropriate to reach high titers. However, due to the nature of this strategy, which includes time intervals where all the substrates may be fully converted (i.e. during DO increases in each DO period), productivity may be inherently limited. To ascertain if productivity could be enhanced, we also tested the effect of constant feeding at the same *p*-CA:glucose ratio using the same strains. In the DO-stat mode, an average of 2 mmol *p*-CA/h (=0.33 g/L/h) was added during the first hours of cultivation. For the constant feeding, we selected a 4-fold higher initial feeding rate (~8 mmol *p*-CA/h = 1.3 g/L/h). In this experiment, KT2440-CJ184 and KT2440-CJ238 accumulated 4-hydroxybenzoate and protocatechuate respectively, which considerably reduced MA yields (**Fig. 2D-E**). In fact, the cultivation with KT2440-CJ184 also exhibited accumulation of *p*-CA at the end of the cultivation. In contrast, KT2440-CJ242 did not accumulate any metabolic intermediate and still produced over 27 g/L of muconate, at 99% yield, and at an increased productivity of 0.53 g/L/h (**Fig. 2F**).

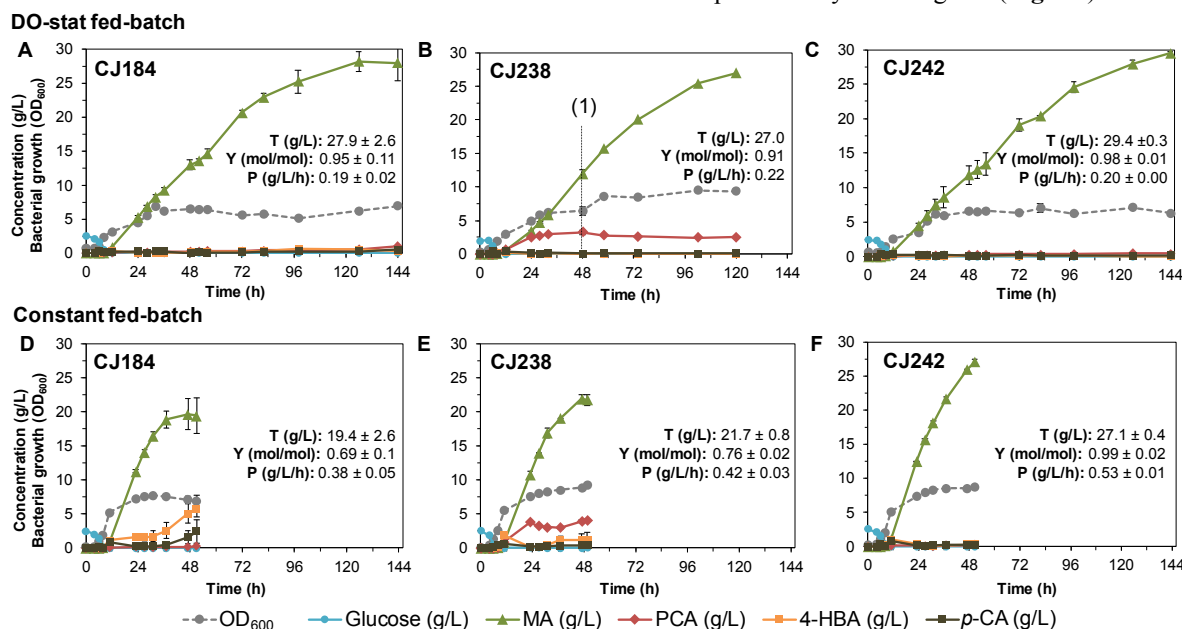


Fig. 2 Muconic acid (MA) production from *p*-coumaric acid (*p*-CA) by engineered *P. putida* KT2440 strains utilizing 2 feeding strategies: (a-c) DO-stat fed batch and (d-f) constant fed-batch. *p*-CA concentration in the feeding bottle was 0.5 M at pH 7. The initial feeding rates for the constant fed-batch was 8 mmol *p*-CA/h. Titrers (T), yields (Y), and productivities (P) are shown in each graph. Each value represents the average of biological duplicates. The error bars represent the absolute difference between the biological duplicates. (1) Time at which one of the biological replicates stopped utilizing glucose and could not be controlled by DO afterwards (see DO profiles, **Fig. S2**). 4-HBA= 4-hydroxybenzoic acid; PCA= protocatechuic acid.

Table 2 Muconic acid titers, yields, and productivities from KT2440-CJ242 and KT2440-CJ518 cultivations at 1:1 vol. batch media:vol. feeding media ratio.

Strain	Initial feeding rates	Titer (g/L)	Yield (mol/mol)	Productivity (g/L/h)
KT2440-CJ242	8 mmol/h (1.3 g/h)	24.9 ^a / 30.5 ^b	0.97 ^a / 0.91 ^b	0.51 ^a / 0.41 ^b
KT2440-CJ242	9 mmol/h (1.5 g/L/h)	24.3 ± 4.8 ^b	0.66 ± 0.30 ^b	0.34 ± 0.07 ^b
KT2440-CJ518	9 mmol/h (1.5 g/L/h)	25.0 ± 6.4 ^b	0.68 ± 0.09 ^b	0.35 ± 0.09 ^b

(a) At 49 h of cultivation.

(b) End-time point (~74 h, feeding depleted).

In light of these results, KT2440-CJ242 was selected to investigate if titer and productivity could be further enhanced. First, the ratio between the initial batch media in the bioreactor and the feeding media (vol:vol) was changed from 3:2 to 1:1. The latter ratio (used in the rest of the study) offers the likelihood of increasing titers in the bioreactors (due to the inability to increase *p*-CA concentration in the feeding media; *p*-CA maximum solubility at neutral pH is 0.5 M). Second, higher feeding rates (9 mmol *p*-CA/h) were also evaluated. The new volume ratio enabled an increased titer, up to 30.5 g/L (Table 2; Fig. S3A) but at a lower yield than that observed before at the same feeding rate at the end of the cultivation (because 4-hydroxybenzoate began to accumulate after 49 h of cultivation, which is the time at which the cultivation was ended previously, Fig. 2F). In addition, productivity was not enhanced at a feeding rate of 9 mmol *p*-CA/h since 4-hydroxybenzoate also accumulated during the cultivation (Table 2; Fig. S3B). Considering the bottleneck observed in 4-hydroxybenzoate, we also overexpressed *PobA* by integrating a second copy of this native gene into the genome of KT2440-CJ242, generating the strain KT2440-CJ518 (Fig. 1, Table S1) and fed *p*-CA at 9 mmol/h.

However, improvements were not observed compared to KT2440-CJ242 (Table 2; Fig. S3C).

These results suggest that approximately a MA titer limit of 25–27 g/L can be achieved at maximum productivities of 0.53 g/L/h while maintaining near-theoretical yields. To understand if these limits are driven by product and/or intermediate toxicity, we subsequently performed toxicity assays with the most relevant molecules in this work.

Evaluation of substrate, metabolic intermediates, and product toxicities in KT2440-CJ242

KT2440-CJ242 was subjected to relevant concentrations of MA, *p*-CA, 4-hydroxybenzoate, and protocatechuate in the presence of glucose, as well as FA and vanillate since these compounds are commonly derived from biomass and were also evaluated in this work (*vide infra*). Increasing MA concentrations (from 5 to 60 g/L) decreased maximum initial growth rates and increased initial lag phases (Fig. 3A). At MA concentrations of 25–30 g/L (the maximum titers reached in the experiments above), the growth rate decreased approximately 30% compared to the control and the lag time doubled. At an initial MA concentration of 60 g/L, bacterial growth was not observed in 24 h cultivations which could indicate the lethal limit. To obtain more information on MA toxicity, we also performed a bioreactor experiment with KT2440-CJ242 utilizing benzoic acid as a substrate (since benzoic acid can be concentrated up to 1 M in the feeding media and the metabolic pathway is shorter than the one from *p*-CA, see Fig. 1) in DO-stat fed batch mode. In this case, maximum MA titers of 52 g/L were achieved. From that point, benzoic acid began to accumulate (Fig. S4). Together, these results suggest that with the current strain, the maximum MA concentrations we can obtain are approximately 50 g/L.

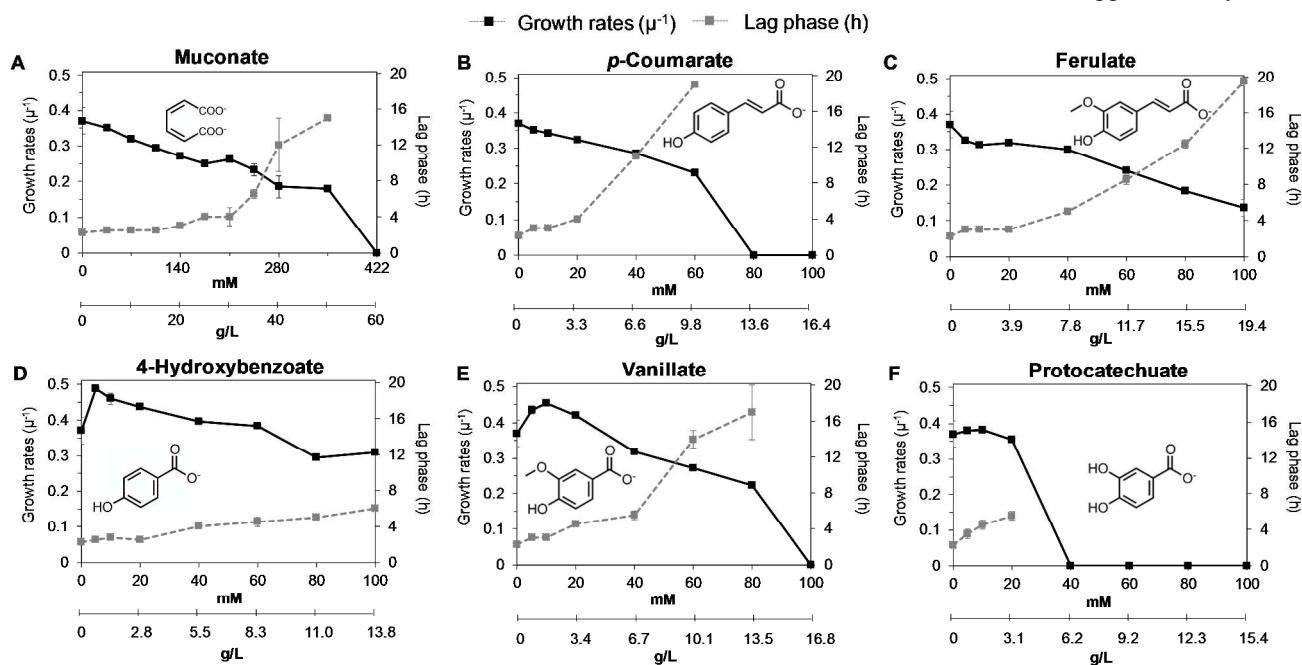


Fig. 3 Maximum growth rates and initial lag phases in KT2440-CJ242 in the presence of initial 5 g/L glucose and different concentrations of (a) muconate, (b) *p*-coumarate, (c) ferulate, (d) 4-hydroxybenzoate, (e) vanillate, (f) and protocatechuate. Values represent the average of two biological replicates and the error bars the absolute difference of that measurement.

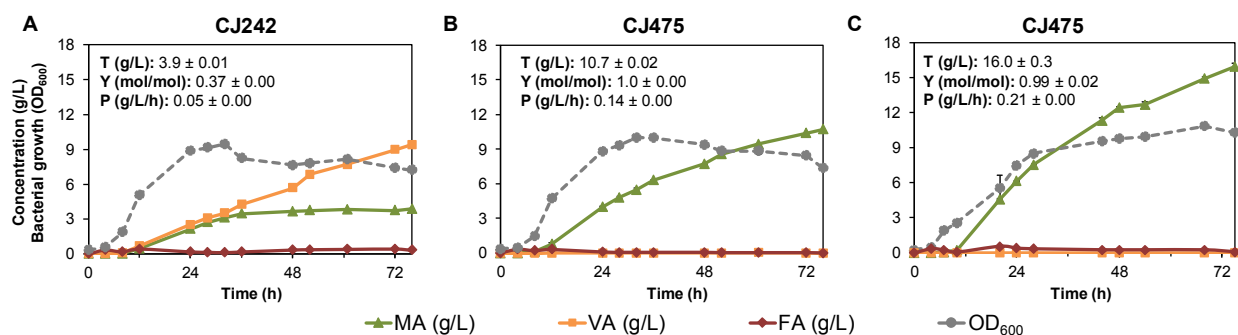


Fig. 4 Muonic acid (MA) production from ferulic acid (FA) in constant fed-batch mode by two different KT2440 strains: (a) KT2440-CJ242 and (b-c) KT2440-CJ475. FA concentration in the feeding bottle was (a, b) 0.16 M and (c) 0.25 M, all at pH 7. The initial feeding rates were approximately (a, b) 2–3 mmol FA/h and (c) 4 mmol FA/h. Titrers (T), yields (Y), and productivities (P) are shown in each graph. Each value represents the average of biological duplicates. The error bars represent the absolute difference between the biological duplicates. VA= vanillic acid.

We also investigated the toxicity of the aromatic compounds used as model substrates in this work (i.e. *p*-CA and FA). FA exhibits higher toxicity than *p*-CA at low concentrations (at 5 and 10 mM) (Fig. 3 B-C). However, *p*-CA shows significantly longer growth lags than FA at concentrations ≥ 40 mM. In fact, growth was not observed at 80 mM *p*-CA, while cells were still able to grow at a FA concentration of 100 mM. In terms of the metabolic intermediates, it is noteworthy that low concentrations (≤ 20 mM) of 4-hydroxybenzoate and vanillate boosted the growth rates compared to the control (only glucose) and that vanillate exhibits higher toxicity than 4-hydroxybenzoate at the highest concentrations. Conversely, protocatechuate exhibits the highest toxicity among the various molecules evaluated in this study and bacterial growth ceased at a concentration between 20 and 40 mM (3 and 6 g/L). This result can help explain the results obtained with KT2440-CJ238 (Fig. 2B-E). Interestingly, protocatechuate was maintained in those cultivations at levels between 3–4 g/L, excluding one case where cells died in one of the bioreactors in DO-stat mode (Fig. 2B), which can potentially be explained by the high toxicity of this intermediate.

MA production from ferulic acid

FA is commonly the second most abundant aromatic compound produced in alkaline treatment of corn stover, and is present at an approximately 3-fold lower concentration than *p*-CA.³⁵ Accordingly, we first evaluated MA production from FA by KT2440-CJ242 at a concentration 3-fold lower in the feeding media than *p*-CA (0.16 M instead of 0.5 M) which resulted in a feeding rate of 2–3 mmol/h (0.5 g FA/L/h). Vanillate was the main product of this cultivation, which substantially decreased MA yields (Fig. 4A). This result suggests that there may be a bottleneck in the vanillate O-demethylase, VanAB (Fig. 1). Thus, we generated another strain, KT2440-CJ475, in which we included another copy of VanAB, driven by the *tac* promoter, which is strong and constitutive in *P. putida*,³⁹ into the genome. In this case, the new strain was able to achieve 100% conversion from FA to MA (Fig. 4B). To investigate the maximum MA titers from FA, we also used a FA feeding source at its maximum solubility at neutral pH (0.25 M). These cultivations lead to a MA production of 16 g/L at a productivity of 0.21 g/L/h. It is also worth highlighting that MA productivities from FA may be still enhanced by increasing feeding rates. However,

considering that this is a less abundant aromatic compound in lignin-rich streams, we did not pursue this optimization.

MA production from mixed aromatic compounds

Lignin streams almost invariably contain a mixture of compounds. To mimic the composition of lignin-rich streams such as alkaline pretreated liquor from corn stover³⁵, we mixed *p*-CA and FA at a relevant molar ratio in the feeding source (0.4 M *p*-CA: 0.1 M FA). In addition, in this experiment, we also wished to evaluate if we could increase MA titers by decreasing feeding rates. As reported above (Table 2), some intermediates such as 4-hydroxybenzoate accumulate at a feeding rate of 8 mmol/h after 49 h of cultivation. Thus, we reduced the feeding rate to 4 mmol/h to investigate if the accumulation of that intermediate was also observed at the same MA concentration. At the highest feeding rate, *p*-CA accumulated rapidly after 49 h, without the accumulation of 4-hydroxybenzoate as observed previously (Fig. 5). MA titers (27 g/L at 49 h) and productivity (0.5 g/L/h at 49 h) were similar to those obtained from *p*-CA at the same rate (Fig. 2F, Table 2). However, at the lowest feeding rate, no intermediates accumulated during the entire cultivation, leading to MA titers of ~ 35 g/L, but at a lower productivity of 0.27 g/L/h. These results again suggest that the catabolism of aromatic compounds slows at MA concentrations between 25–30 g/L MA and that it is possible to avoid the accumulation of metabolic intermediates and/or substrate by decreasing feeding rates.

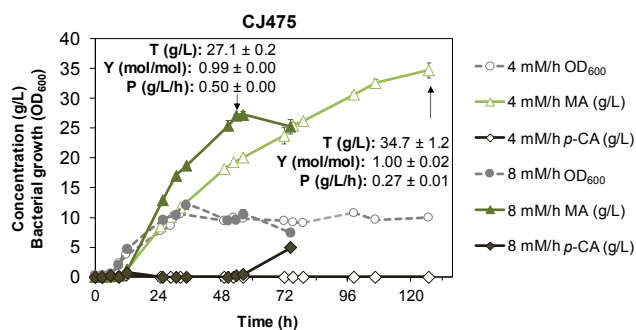


Fig. 5 Muonic acid (MA) production from a mix of *p*-coumaric acid (*p*-CA) and ferulic acid (FA) in constant fed-batch mode by KT2440-CJ475 at two different initial feeding rates, 4 and 8 mmol/h. *p*-CA and FA concentrations in the feeding bottle were 0.4 M and 0.1 M, respectively. Titrers (T), yields (Y), and productivities (P) are shown in each graph. Each value represents the average of biological duplicates. The error bars represent the absolute difference between the biological duplicates.

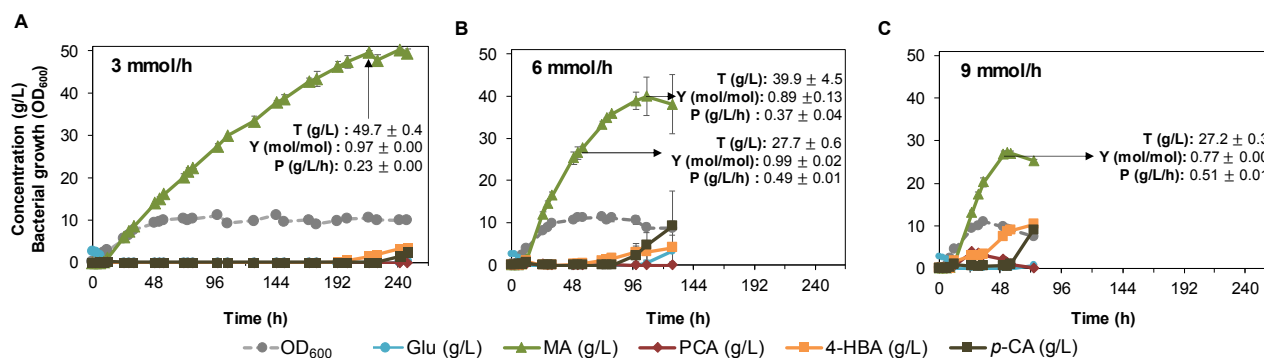


Fig. 6 Muonic acid (MA) production from *p*-coumaric acid (*p*-CA) in constant fed-batch mode by KT2440-CJ242 at three different initial feeding rates: (a) 3 mmol *p*-CA/h, (b) 6 mmol *p*-CA/h, and (c) 9 mmol *p*-CA/h. *p*-CA concentration in the feeding bottle was 0.75 M at pH 9.5. Titer (T), and yields (Y) and productivities (P) are shown in each graph and arrows highlight the time points in which maximum T and Y were achieved. Each value represents the average of biological duplicates. The error bars represent the absolute difference between the biological duplicates. 4-HBA= 4-hydroxybenzoic acid; PCA= protocatechuic acid.

High pH feeding enables higher MA titers from *p*-CA

Considering that the lignin streams we are highlighting in this work are alkaline in nature (Fig. 1), we evaluated the possibility of feeding high pH (pH ~9.5) solutions of aromatic compounds. This feeding strategy presents several potential advantages: (1) lignin streams would not need to be neutralized *a priori*, which would reduce the overall salt burden in wastewater treatment, (2) it would theoretically decrease the dilution effect resulting from the addition of base in the bioreactor, and (3) it would allow higher substrate concentrations since lignin and aromatic compounds are more soluble at higher pH. The last two points could then also enable higher titers. The maximum solubilities at pH=9.5 for *p*-CA and FA are 0.75 M and 0.5 M, respectively. However, in the case of FA, we observed a rapid FA degradation at that pH.

Due to the instability of FA, we tested this feeding strategy only with *p*-CA and KT2440-CJ242 (since the overexpression of VanAB is not necessary in this case) at three different feeding rates (3, 6, and 9 mmol *p*-CA/h). At the lowest feeding rate, we achieved almost complete conversion of *p*-CA to MA at the end of the cultivation (Fig. 6A). The titer and productivity obtained in this run were similar to those obtained from benzoic acid (Fig. S4) and, in both cases, metabolic intermediates accumulate at the same MA concentration (approximately 50 g/L), likely due to the MA toxicity (Fig. 3A).

At the intermediate feeding rate, we observed similar results to those presented in the previous sections (Fig. 2F, Fig. 5). Although the feeding rates are lower (6 mmol/h instead of 8 mmol/h), due to the reduction in base dilution, we reached a similar titer and productivity (28 g/L and 0.5 g/L/h) at the same time point (approximately 49 h) before intermediates accumulate. However, utilizing this feeding strategy, MA titers reached almost 40 g/L at a productivity of 0.37 g/L/h and 89% yield (Fig. 6B). Conversely, at the highest feeding rate, 4-hydroxybenzoate progressively accumulated from the beginning of the cultivation. Overall, this experiment reaches the highest MA titers reported to date to our knowledge from *p*-CA and demonstrate that high-pH feeding may a viable feeding strategy to feed alkaline lignin streams in the bioreactors.

Muonic acid production from high-pH lignin streams

In this work, we focus on lignin streams that are derived from a biorefinery process from corn stover²⁴ (Fig. 7A). The pretreatment process consists of deacetylation and mechanical-refining steps.²⁴ The deacetylation process uses a mild alkaline treatment which generates an aqueous lignin-rich stream dubbed alkaline pretreated liquor (APL). Then, the solids are enzymatically hydrolyzed to release soluble monomeric sugars and the remaining solid fraction (high-lignin content residue⁴⁰) can be further solubilized through base catalyzed depolymerization (BCD), as reported previously.^{21, 41} Both APL and the lignin liquor resulting from the BCD process (dubbed BCDL) contain *p*-CA and FA as the most abundant aromatic compounds. Because BCDL contains a low FA concentration in proportion to *p*-CA compared to APL (Fig. 7A), we selected KT2440-CJ242 and KT2440-CJ475 for the conversion of BCDL and APL, respectively. These cultivations were initiated as in previous experiments, a batch phase in minimal media and then a fed-batch phase where in this case the lignin streams (250 mL) were fed at 4 mL/h. As expected, due to the higher concentration of aromatic compounds in BCDL, MA titers were higher in BCDL (3.7 g/L) than in APL (0.65 g/L) (Fig. 7B,C). The cell densities obtained in these experiments were higher (OD₆₀₀ = ~16) than those reached in the model compound experiments (OD₆₀₀ = ~10), even though the glucose amount added was the same in all cases. This result is likely due to the presence of other carbon sources in the lignin streams such as acetate and carboxylic acids, as previously reported.^{36, 42, 43}

As expected, MA productivities in the lignin streams are relatively low (0.06 g/L/h). However, the feeding rates were not optimized in this experiment and could likely be increased. Interestingly in both cases, MA yield (calculated as MA mol/(*p*-CA+FA) mol) was higher than 100%. This result indicates that there are other aromatic compounds that lead to MA production that we do not detect and/or that *P. putida* is able to break down oligomeric lignin and convert it to MA.³⁶ To gain further insights into lignin modification by the bacterium, we analyzed changes in the molecular weight (MW) of lignin, by gel permeation chromatography at the end

of the cultivation and compared it with the initial lignin profiles. The results indicate (Fig. S5) that low MW lignin in BCDL was almost completely utilized by the bacterium. However, in APL, although the main two low MW lignin peaks disappear, a new low MW peak appears after the bacterial treatment, suggesting that *P. putida* may be also releasing other low MW compounds that it cannot natively utilize. Future studies will focus on identifying these metabolites to better understand lignin breakdown by *P. putida*. For the high MW lignin, we did not observe considerable changes after 64 h of cultivation. Overall, 15% of the lignin was converted to MA in both cases (g MA/g lignin).

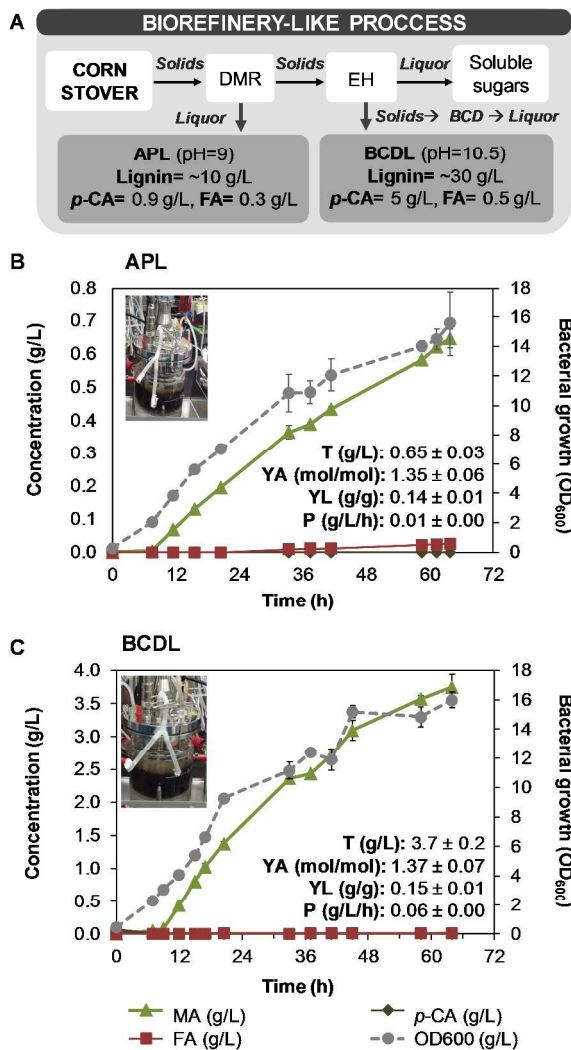


Fig. 7 Muconic acid (MA) production from lignin streams. (a) Overview of lignin stream generation from a corn stover-based biorefinery process. MA production from (b) alkaline pretreated liquor (APL) by KT2440-CJ475 and (c) solubilized lignin liquor from a base catalyzed depolymerization process (BCDL) by KT2440-CJ242. Ferulic acid (FA) and *p*-coumaric acid (*p*-CA) concentrations in APL are 0.3 g/L and 0.9 g/L, respectively. FA and *p*-CA concentrations in BCDL are 0.5 g/L and 5.0 g/L, respectively. Titrers (T), yields from aromatics (YA) and from initial lignin source (YL), and productivity (P) are shown in each graph. The error bars represent the absolute value difference of two biological replicates. BCD= base catalyzed depolymerization; DMR= deacetylation and mechanical refining; EH= enzymatic hydrolysis.

Discussion

Decades of metabolic engineering and fermentation process development have been invested into the conversion of sugars to fuels and value-added chemicals at high titers, rates, and yields – critical economic parameters for the development of any bioprocess. The advent of microbial lignin conversion strategies will warrant a similar level of effort to develop robust strains and bioprocesses to achieve the same level of success for a biological approach to lignin valorization. A critical point to start this development focuses on process configuration. For instance, performing bioreactor cultivations relative to shake flask experiments can lead to more realistic information on the limitation of the biocatalysts and allows for improved understanding of substrate, product, or intermediate toxicity when microbial systems are challenged to achieve industrially-relevant titers, yields, and productivities.

Lignin deconstruction to bioavailable compounds remains one of the most important challenges in enabling biological lignin valorization, since bacteria studied to date cannot rapidly utilize high molecular weight lignin, which is typically a large fraction in many lignin streams.¹⁵ Thus, biological and/or catalytic processes, focused on generating higher yields of bioavailable monomeric aromatic compounds from lignin, need to continue being developed to make the technology presented in the current work a realistic, cost effective strategy. Despite not yet having monomer-rich lignin streams, we have demonstrated 15% lignin conversion to MA (g MA/g lignin) from two streams. As shown in Fig. 7, MA yields from detectable monomeric species in these lignin streams is over 100%, and titers approach 4 g/L in one case. However, it is noteworthy that MA titers could be increased by starting the cultivation directly in lignin (instead of minimal media) and/or concentrating lignin streams (as recently shown by Kohlstedt et al.²⁶).

Beyond increasing bioavailable compounds in the lignin streams, the limitations of the biological catalysts – in our case engineered *P. putida* KT2440 – must be understood in terms of substrate, intermediate, or product toxicity limits to select an appropriate bioreactor cultivation strategy for MA production. As presented in the current study, the major aromatic deconstruction product from corn stover (*p*-CA) is toxic at relatively low concentrations: 60 mM (~10 g/L) decreases growth rates by 34% and 80 mM (~14 g/L) was lethal for the bacterium (Fig. 3B). The same reduction in growth rate was recently reported for the native *P. putida* KT2440,³⁸ which demonstrates that the toxicity effect does not vary in both native and the MA-producing strains studied here. Due to the toxicity of this substrate, we initially selected a DO-stat fed-batch feeding strategy and demonstrated that it enables high titers, but at the expense of lower productivity. Thus, we then evaluated a constant feeding strategy at a higher *p*-CA feeding rate but still at a low *p*-CA toxic concentration (8 mmol *p*-CA/h) and showed a ~2.5-fold MA productivity increase (to 0.53 g/L/h) while still maintaining 100% MA yields (Fig. 2). MA productivity from catechol and benzoic acid has been reported to be as high as 5.5 g/L/h (Table 1)^{25, 28}, but both the substrates (which are in a shorter pathway to MA, 1 or 2 enzyme steps instead of 7) and the feeding strategy (constant fed-batch with cell recycle in the

benzoate cases) can have important effects on the productivity value.

FA, a less toxic substrate than *p*-CA, was also evaluated as a model compound in bioreactors for MA production. We first employed the strain KT2440-CJ242 for conversion purposes. Even though this strain has a global catabolic repressor knocked out, which has been reported to enhance VanAB production,²³ it was unable to overcome the bottleneck in vanillate. The overexpression of VanAB has been previously reported to enhance vanillate utilization rates in a different *P. putida* strain.⁵² Here, we also overexpressed VanAB and observed complete conversion to MA.

In our attempts to increase MA productivity by increasing feeding rates of *p*-CA, we discovered another limitation of engineered *P. putida* KT2440 strains: 4-hydroxybenzoate accumulates, even though further metabolic engineering was applied in an attempt to alleviate that bottleneck by overexpressing Poba (**Table 2**). It is unclear, however, how substantial the improvement would be if this bottleneck was removed. To understand whether aromatic compound transport might be another limitation, we performed a preliminary experiment with KT2440-CJ242 in which *p*-CA was fed at 10, 11, and 12 mmol/h (**Fig. S6**). At 10 and 11 mmol/h, both MA and 4-hydroxybenzoate accumulate. However, at 12 mmol/h, *p*-CA accumulated from the beginning of the cultivation, which indicates that transport may be already a subsequent bottleneck. Utilizing a feeding rate of 12 mmol/h and assuming 100% conversion, MA productivities could only achieve approximately 0.85 g/L/h. Considering the need to reach productivities up to 1 g/L/h (a value that would approach industrial relevance), adaptive laboratory evolution (to accelerate the overall utilization rates, potentially including improved transport of aromatic substrates), directed evolution (to improve certain enzymes), protein engineering, or additional metabolic engineering would need to be leveraged to enable better utilization and/or transport of these aromatic substrates. Additional approaches such as employing functional biosensors (as recently described in *P. putida*)⁴⁴ to allow high-throughput strain evaluation and isolation of evolved populations toward improving enzymes and metabolic pathways could also prove useful to this end.

Native *P. putida* KT2440 has been described as highly tolerant to toxic substrates (i.e. *p*-CA or catechol) compared to other organisms because of its membrane composition, efflux pumps, motility, or the higher generation of NADPH by utilizing the Entner-Doudoroff, Embden-Merhof-Parnas pathway.^{29, 38, 45} However, these tolerance mechanisms may be insufficient to maintain efficient metabolism in the presence of high MA concentrations. Thus, product toxicity may also lead to reduced MA productivity and the amplification of some of the bottlenecks detailed above. As shown in **Fig. 3**, even though MA is less toxic than the aromatic substrates or metabolic intermediates, it is still likely an important toxicity driver. Specifically, MA maximum titers of approximately 50 g/L have been corroborated in several experiments in the current study (**Fig. 3A, Fig. 6A, Fig. S4**). MA toxicity has been also evaluated in a different MA-producing strain

(KT2440-JD1) by van Duuren *et al.*,²⁹ and the trends are quite similar to those observed here, suggesting a general toxicity threshold for *P. putida*. For instance, at a MA concentration of 300 mM (~40 g/L), maximum growth rates decrease 50% in both cases. van Duuren *et al.* also reported that benzoic acid uptake rates begin to decline at MA concentrations between 15-20 g/L and decrease 75% at concentrations close to 30 g/L.²⁹ This finding relates to our observations regarding different feeding rates: low feeding rates allow for full conversion of substrates or metabolic intermediates when MA concentration are higher than 25-30 g/L (**Fig. 5, Fig. 6**). Some effects of high MA concentrations and other toxic compounds on the cells may be related to reduced activity of enzymes in the β -ketoacid pathway²⁸ and on energy shortages provoked by the disruption of the membrane potential and inhibition of oxidative phosphorylation.^{46, 47} Thus, to improve MA production from lignin streams, we need to enhance the tolerance of *P. putida* to higher MA concentrations. For this purpose, adaptive laboratory evolution can be useful, which will be pursued in future studies, alongside targeted engineering strategies. For instance, the constitutive overexpression of the chaperone genes, *groEL*, *groES*, and *clpB* (which increased the tolerance of *P. putida* to pyrolysis wastewater streams up to 200-fold),⁴⁸ the engineering of the phospholipid composition in the membrane of *E. coli* (which improved the tolerance and production of a variety of molecules),⁴⁹ and the overexpression of efflux pumps (which are found in highly solvent tolerant bacteria)⁵⁰ could be also applied to our current bacterial strains.

Apart from pathway, enzyme, or protein engineering to overcome bottlenecks and/or increase the tolerance to product, it is clear that modifications in the feeding strategy can enhance the process performance. For instance, the addition of glucose pulses has been reported to overcome the accumulation of catechol during MA production, likely due to an increase in ATP production.²⁶ Similarly, our work has also shown that a minimum level of glucose, or generally a carbon and energy source, is necessary to fully convert MA from *p*-CA without the accumulation of any metabolic intermediates (**Fig. S1**). The catabolism of *p*-CA and FA to MA only releases a single acetyl-CoA, which is likely not enough to support the bacterial metabolism for a bioprocess without any additional carbon and energy source. However, a promising glucose-free process for the production of MA has been recently reported by Sonoki *et al.*,³³ but titers, yields, and productivity would need to be substantially enhanced to be a competitive process. Currently, glucose and other sugars are readily obtained in a biorefinery process. Indeed, a fraction of the glucose could also potentially be simultaneously directed to MA production.^{13, 51} In addition, lignin-rich streams such as APL also contain high concentrations of acetate and other carboxylic acids^{36, 42} that could be used as a carbon source and support MA production.²³ Further research in bioprocess optimization utilizing these alternative carbon sources will be conducted in future work to enhance the overall conversion to MA.

Conclusion

MA is a promising chemical building block that can be produced with high atom efficiency from lignin. As shown in the current work, parallel strain and bioreactor process development revealed bottlenecks and limitations of the system, which enabled considerable improvements to MA production by engineered *P. putida* KT2440. This work represents progress towards the goal of industrially relevant conversion of lignin-derived aromatic monomers to MA. Continued process development and engineering *P. putida* for better product tolerance and higher productivity will be pursued in future work.

Materials and Methods

Recovery of lignin streams

The lignin streams utilized in the current study derive from the biorefinery process designed at NREL by Chen et al.²⁴ with some modifications. For the production of APL for the bioreactor experiments, 15 g of corn stover were mixed with 150 mL of a 0.7% NaOH solution into stainless steel 200 mL reactors. The reaction was carried out at 130°C for 30 min. Then, the reactors were quenched and the mixture centrifuged at 8,000 rpm in sterile conditions. The supernatant (at pH 9) was directly used as feeding in the bioreactor experiments. For the production of BCDL, dry solid material remaining from the enzymatic hydrolysis step was added as 10% (w/v) solids to a 2% NaOH solutions and loaded into 200 mL stainless steel reactors as previously reported.²¹ The reaction was carried out at 120°C for 30 min. In this case, the solubilized material was directly used as feeding without any centrifugation step for the bioreactor experiments.

Strains and plasmid construction

P. putida KT2440 (ATCC 47054) strains were constructed as previously described.⁵³ Specific strain construction details are provided in Table 3 and SI (SI materials and methods, Table S1, Table S2, Table S3).

Table 3. Genotypes of the strains used in this study.

Strain	Genotype
KT2440-CJ184	<i>P. putida</i> KT2440 Δ catRBC::Ptac:catA Δ pcaHG::Ptac:aroY:ecdB:ecdD
KT2440-CJ238	<i>P. putida</i> KT2440 Δ catRBC::Ptac:catA Δ pcaHG::Ptac:aroY:ecdB:asbF Δ crc
KT2440-CJ242	<i>P. putida</i> KT2440 Δ catRBC::Ptac:catA Δ pcaHG::Ptac:aroY:ecdB:ecdD Δ crc
KT2440-CJ475	<i>P. putida</i> KT2440 Δ catRBC::Ptac:catA Δ pcaHG::Ptac:aroY:ecdB:ecdD Δ crc ffpvA::Ptac:vanAB
KT2440-CJ518	<i>P. putida</i> KT2440 Δ catRBC::Ptac:catA Δ pcaHG::Ptac:aroY:ecdB:ecdD Δ crc ffpvA::Ptac:pobA

Seed preparation

To revive strains from glycerol stocks, the surface of the vials were scrapped and inoculated in 250 mL baffled flasks containing 50 mL LB media. These cultures (seed cultures) were incubated overnight at 30°C and 225 rpm. The cells were then washed and concentrated in 5 mL of modified minimal media (M9) for inoculation in the bioreactors at an initial OD₆₀₀ of 0.2. The M9 media consists of 13.55 g/L Na₂HPO₄, 6 g/L KH₂PO₄, 1 g/L NaCl, 2.25 g/L (NH₄)₂SO₄, 2 mL/L from 1 M MgSO₄, 0.1 mL/L from 1 M CaCl₂, and 1 mL/L from 18 mM FeSO₄.

Batch-phase: media preparation and bioreactor control

The media utilized in the batch phase was the same in all the experiments carried out in this study, which contained M9 and 2.7 g/L (15 mM) glucose as a carbon and energy source. The volume of the batch media was 250 or 300 mL, depending on the experiment (detailed below). The bioreactors used in this study were 0.5 L BioStat-Q Plus bioreactors (Sartorius Stedim Biotech) and were controlled at 30°C, at pH 7 with 4 N NaOH, and sparged with air at 1 vvm. The initial agitation in the batch phase was 350 rpm. When the saturation of oxygen reached approximately 30%, the agitation was manually increased 50 rpm (in general 6-7 times). Once the glucose was depleted in the batch phase, indicated as a rapid increase in DO levels (up to 75%), the fed-batch phase was initiated (see details below). It is also worth noting that at 4 h, aromatic compounds were added in the bioreactor to induce a metabolic switch in *P. putida* in the exponential growth phase. Specifically we added 2 mM *p*-CA when *p*-CA was the feeding source, 2 mM FA when FA was the feeding source, 1 mM *p*-CA and 1 mM FA when both *p*-CA and FA were the feeding source, and 4 mL of the corresponding lignin stream when actual streams were the feeding source. Bioreactor experiments were performed in duplicate and samples (1.5 mL) were taken periodically to analyze bacterial growth (OD₆₀₀) and the different metabolites. The ammonium concentration was also analyzed by YSI (YSI 7100 MBS) in various bioreactor cultivations and the values were over 0.2 g/L during the entire fed-batch phase (data not shown). The model aromatic compounds *p*-CA and FA were obtained from AKSci (AK Scientific) and Sigma-Aldrich, respectively

Fed-batch phase: media preparation and feeding strategies

DO-stat fed-batch with *p*-CA at neutral pH. The feeding media (200 mL) contained 85 g/L (0.5 M) *p*-CA, 45 g/L glucose, and 9 g/L (NH₄)₂SO₄, and 6mL/L antifoam 204 (Sigma). The solution was adjusted to pH 7 with 10 N NaOH. As detailed above, when the glucose in the batch phase was depleted (batch volume of 300 mL), the fed-batch was initiated. Specifically, the feeding solution was pumped for 30 s intervals (□0.8 mL, bringing the concentration in the bioreactor to 1.3 mM *p*-CA and 0.66 mM glucose) every time that the DO reached a value of 75%. The agitation was manually adjusted to maintain DO minimal values over 10%. Bioreactor experiments were concluded when the feeding was fully consumed or DO did not decrease anymore after adding feeding solution (this fact also applies to the experiments below).

Constant fed-batch with *p*-CA at neutral pH. The feeding media (200 or 250 mL, as detailed in the Results section) contained 85 g/L (0.5 M) *p*-CA, 45 g/L glucose, and 9 g/L (NH₄)₂SO₄, and 6mL/L antifoam 204. The solution was adjusted to pH 7 with 10 N NaOH. Once the batch phase (containing 300 or 250 mL of media, detailed in the Results section) was terminated, the feeding solution was constantly added at an initial feeding rate of 8 mM *p*-CA/h. The DO was automatically controlled by agitation at a DO level of 30-35% (this parameter applies to all the constant feeding experiments). We based this DO control on work from Choi et al., which reported that higher DOs than 30-40% do not enhance MA productivity.²⁸

Constant fed-batch with FA at neutral pH. The feeding media (250 mL) contained 31 g/L or 48.5 g/L (0.16 or 0.25 M, respectively) FA, 45 g/L glucose, and 9 g/L (NH₄)₂SO₄, and 6 mL/L antifoam 204. The solution was adjusted to pH 7 with 10 N NaOH. Once the batch phase (containing 250 mL of media) was terminated, the feeding solution was constantly added to reach at an initial feeding rate of 2-3 or 4 mmol FA/h.

Constant fed-batch with mixed *p*-CA and FA at neutral pH. The feeding media (250 mL) contained 19.4 g/L (0.1 M) FA and 65.6 g/L (0.4 M) *p*-CA, 45 g/L glucose, and 9 g/L (NH₄)₂SO₄, and 6 mL/L antifoam 204. The solution was adjusted to pH 7 with 10 N NaOH. Once the batch phase (containing 250 mL of media) was terminated, the feeding solution was constantly added to reach at an initial feeding rate of 4 or 8 mmol (*p*-CA+FA)/h.

Constant fed-batch with *p*-CA at high pH. The feeding media (250 mL) contained 123 g/L (=0.75 M) *p*-CA, 67.5 g/L glucose, and 13.5 g/L (NH₄)₂SO₄, and 6 mL/L antifoam 204. The solution was adjusted to pH 9.5 with 10 N NaOH. Once the batch phase (containing 250 mL of media) was terminated, the feeding solution was constantly added to reach an initial feeding rate of 3, 6, and 9 mmol *p*-CA/h. Fresh feeding for these cultivations was prepared every 3 days of cultivation.

Constant fed-batch of lignin streams at high pH. The feeding media (250 mL) contained 227.5 mL high pH lignin stream (APL or BCDL) and 22.5 mL of concentrated glucose and (NH₄)₂SO₄ to yield a final concentrations of 45 g/L and 9 g/L, respectively. The feeding solution was added at a rate of 4 mL/h.

Calculation of fermentation parameters

MA titers (g/L) correspond to the concentration at the end of the cultivation (or as otherwise indicated). Yields (mol/mol) are calculated as mol of MA between mol of aromatic compounds (pure or detected in the lignin stream). Productivity (g/L/h) is calculated as MA concentration divided by the total duration of the cultivation (as otherwise indicated).

Toxicity assays in Bioscreen C

To evaluate the toxicity of the different aromatic compounds and MA, we employed a 'Bioscreen-C™ Automated Microbiology Growth Curves Analysis System' to track the bacterial growth through OD₆₀₀ measurements during 24 h of cultivation. The seed culture with KT2440-CJ242 was prepared as described above. Then, cells were washed with M9 and inoculated to each well (5 μL) to yield an initial OD₆₀₀ of 0.1. Each well contained M9 supplemented with 5 g/L glucose and the corresponding molecule at different concentrations. Specifically, *p*-CA, FA, protocatechuic acid, vanillic acid, and 4-hydroxybenzoic acid were solubilized with NaOH to yield a concentration of 200 mM and pH 7 and then added to each well at final concentrations of 20, 40, 60, 80, 100 mM in 2-fold concentrated M9. MA was prepared at an initial concentration of 80 g/L, also a pH 7, and mixed with 4-fold concentrated M9 at concentrations of 5, 10, 15, 20, 25, 30, 35, 40, 50, and 60 g/L. The plates were incubated at 30°C in the

equipment and shaken continuously at medium speed. Maximum growth rates (μ⁻¹) and initial lag phases (h) were calculated from each growth curve. Each condition was performed in duplicate.

Analytical methods

Model aromatic compound quantitation. Metabolite analysis from those cultivations involving model aromatic compounds was performed on an Agilent 1100 series HPLC system, including a refractive index detector and a diode array detector (DAD) (Agilent Technologies). Analysis was performed by injecting 6 μL of 0.02 μm filtered culture supernatant onto a Phenomenex Rezex™ RFQ-Fast Acid H⁺(8%) column with a cation H⁺guard cartridge (Bio-Rad Laboratories) at 85°C using a mobile phase of 5 mM sulfuric acid at a flow rate of 1.0 mL/min.

MA and aromatic compound quantitation in BCDL.

Metabolite analysis in BCDL was performed on an Agilent 1100 HPLC system equipped with a DAD and an Ion Trap SL (Agilent Technologies) MS with in-line electrospray ionization (ESI). Each sample was injected at a volume of 25 μL into the LC/MS system. Compounds were separated using a Develosil C30 RPaqueous, 5 μm, 4.6 × 250 mm column (Phenomenex) at an oven temperature of 30°C. The chromatographic eluents consisted of A) water modified with 4mM ammonium formate, and B) acetonitrile/water (9:1, v/v) also modified with 4mM ammonium formate. At a flow rate of 0.7 mL/min, the eluent gradient was as follows: initially, 0% B; going to 7% B at 13 min; 18 min, 10% B; 25 min, 15% B; 52.1 min, 100% B which was held for 10 min before equilibrium for a total run time of 45 min. Flow from the HPLC-DAD was directly routed in series to the ESI-MS ion trap. The DAD was used to monitor chromatography at 210, 225, and 325 nm for a direct comparison to MS data. MS and MS/MS parameters are as follows: smart parameter setting with target mass set to 165 Da, compound stability 10%, trap drive 50%, capillary at 3500 V, fragmentation amplitude of 0.75 V with a 30 to 200% ramped voltage implemented for 50 msec, and an isolation width of *m/z* 2 (He collision gas). The ESI nebulizer gas was set to 60 psi, with dry gas flow of 11 L/min held at 350°C. Into each sample and standard mixture, 0.01 g/L 3,4-dihydroxybenzaldehyde (97% purity, Sigma Aldrich) was added to adjust for chromatographic shift and detector response. MS scans and precursor isolation-fragmentation scans were performed across the range of 40-750 Da. Standards of protocatechuic acid, *cis,cis*-MA, *p*-CA, vanillic acid, 4-hydroxybenzoic acid, and FA were purchased from Sigma Aldrich and used to construct calibration curves between the ranges of 1 – 100 μg/L. A minimum of five calibration levels was used with an r² coefficient of 0.995 or better for each analyte.

MA and aromatic compound quantitation in APL.

Metabolite analysis in APL was performed on an Agilent 1200 LC system (Agilent Technologies) equipped with a DAD. Each sample and standard was injected at a volume of 10 μL onto a Phenomenex Luna C18(2) column 5 μm, 4.6 × 150 mm column (Phenomenex). The column temperature was maintained at 30°C and the buffers used to separate the analytes of interest were A) 0.05% acetic acid in water and B)

0.05% acetic acid in acetonitrile. The chromatographic separation was carried out using a gradient of: initially starting at 1% B going to 50% B at 35 min before immediately switching to 99% B at 35.1 min, before equilibrium for a total run time of 47 min. The flow rate of the mobile phases was held constant at 0.6 mL/min. The same standards used in the BCDL experiments were also used to construct calibration curves, but between the ranges of 5 – 200 µg/L. Three separate wavelengths from the DAD were used to identify and quantitate the analytes of interest. A wavelength of 210 nm and 225 nm was used for analytes protocatechuic acid, vanillic acid, 4-hydroxybenzoic acid, and *cis, cis*-MA. A wavelength of 325 nm was used for analytes *p*-CA, and FA. A minimum of five calibration levels was used with an r^2 coefficient of 0.995 or better for each analyte.

Abbreviations

References

1. T. Polen, M. Spelberg and M. Bott, *J. Biotechnol.*, 2013, **167**, 75-84.
2. K. M. Draths and J. W. Frost, *J. American Chem. Soc.*, 1994, **116**, 399-400.
3. N.-Z. Xie, H. Liang, R.-B. Huang and P. Xu, *Biotechnol. Adv.*, 2014, **32**, 615-622.
4. D. R. Vardon, M. A. Franden, C. W. Johnson, E. M. Karp, M. T. Guarnieri, J. G. Linger, M. J. Salm, T. J. Strathmann and G. T. Beckham, *Energy Environm. Sci.*, 2015, **8**, 617-628.
5. W. Schutyser, T. Renders, S. Van den Bosch, S. F. Koelewijn, G. T. Beckham and B. F. Sels, *Chem. Soc. Rev.*, 2018, **47**, 852-908.
6. M. Suastegui, J. E. Matthiesen, J. M. Carraher, N. Hernandez, N. Rodriguez Quiroz, A. Okerlund, E. W. Cochran, Z. Shao and J.-P. Tessonnier, *Ang. Chemie Int. Ed.*, 2016, **55**, 2368-2373.
7. N. A. Rorrer, J. R. Dorgan, D. R. Vardon, C. R. Martinez, Y. Yang and G. T. Beckham, *ACS Sust. Chem. Eng.*, 2016, **4**, 6867-6876.
8. N. A. Rorrer, D. R. Vardon, J. R. Dorgan, E. J. Gjersing and G. T. Beckham, *Green Chemistry*, 2017, **19**, 2812-2825.
9. B. H. Shanks and P. L. Keeling, *Green Chem.*, 2017, **19**, 3177-3185.
10. C. Weber, C. Brückner, S. Weinreb, C. Lehr, C. Essl and E. Boles, *Appl. Env. Microb.*, 2012, **78**, 8421-8430.
11. K. A. Curran, J. M. Leavitt, A. S. Karim and H. S. Alper, *Metab. Eng.*, 2013, **15**, 55-66.
12. V. Bui, M. K. Lau, D. Macrae and D. Schweitzer, *US patent US8809583B2*, 2013.
13. C. W. Johnson, D. Salvachúa, P. Khanna, H. Smith, D. J. Peterson and G. T. Beckham, *Metab. Eng. Commun.*, 2016, **3**, 111-119.
14. A. J. Ragauskas, G. T. Beckham, M. J. Bidy, R. Chandra, F. Chen, M. F. Davis, B. H. Davison, R. A. Dixon, P. Gilna, M. Keller, P. Langan, A. K. Naskar, J. N. Saddler, T. J. Tschaplinski, G. A. Tuskan and C. E. Wyman, *Science*, 2014, **344**.
15. G. T. Beckham, C. W. Johnson, E. M. Karp, D. Salvachúa and D. R. Vardon, *Curr. Opin. Biotechnol.*, 2016, **42**, 40-53.
16. R. Davis, L. Tao, E. C. D. Tan, M. J. Bidy, G. T. Beckham, C. Scarlata, J. Jacobson, K. Cafferty, J. Ross, J. Lukas, D. Knorr and P. Schoen, *Technical Report. NREL/TP-5100-60223*, 2013.
17. A. Corona, M. J. Bidy, D. R. Vardon, M. Birkveda, M. Hauschilda and G. T. Beckham, *Green Chem.*, 2018, **In print**.
18. C. Xu, R. A. D. Arancon, J. Labidi and R. Luque, *Chem. Soc. Rev.*, 2014, **43**, 7485-7500.
19. F. Paola and R. Roberto, *Ang. Chemie Int. Ed.*, 2014, **53**, 8634-8639.
20. J. Zakzeski, P. C. A. Bruijninx, A. L. Jongerius and B. M. Weckhuysen, *Chem. Rev.*, 2010, **110**, 3552-3599.
21. A. Rodriguez, D. Salvachúa, R. Katahira, B. A. Black, N. S. Cleveland, M. Reed, H. Smith, E. E. K. Baidoo, J. D. Keasling, B. A. Simmons, G. T. Beckham and J. M. Gladden, *ACS Sust. Chem. Eng.*, 2017, **5**, 8171-8180.
22. T. Sonoki, M. Morooka, K. Sakamoto, Y. Otsuka, M. Nakamura, J. Jellison and B. Goodell, *J. Biotechnol.*, 2014, **192 Pt A**, 71-77.
23. C. W. Johnson, P. E. Abraham, J. G. Linger, P. Khanna, R. L. Hettich and G. T. Beckham, *Metab. Eng. Commun.*, 2017, **5**, 19-25.
24. X. Chen, E. Kuhn, E. W. Jennings, R. Nelson, L. Tao, M. Zhang and M. P. Tucker, *Energy Environm. Sci.*, 2016, **9**, 1237-1245.
25. A. Kaneko, Y. Ishii and K. Kirimura, *Chem. Lett.*, 2011, **40**, 381-383.

Acknowledgements

This work was authored by Alliance for Sustainable Energy, LLC, the manager and operator of the National Renewable Energy Laboratory for the U.S. Department of Energy (DOE) under Contract No. DE-AC36-08GO28308. Funding was provided by the U.S. Department of Energy Office of Energy Efficiency and Renewable Energy Bioenergy Technologies Office. We thank Rui Katahira for conducting the GPC analysis and William Michener for helpful discussions on lignin analytics.

26. M. Kohlstedt, S. Starck, N. Barton, J. Stolzenberger, M. Selzer, K. Mehlmann, R. Schneider, D. Pleissner, J. Rinkel, J. S. Dickschat, J. Venus, B. J. H. v. D. J and C. Wittmann, *Metab. Eng.*, 2018, **47**, 279-293.
27. J. Becker, M. Kuhl, M. Kohlstedt, S. Starck and C. Wittmann, *Microb. Cell Fact.*, 2018, **17**, 115.
28. W. J. Choi, E. Y. Lee, M. H. Cho and C. Y. Choi, *J. Ferment. Bioeng.*, 1997, **84**, 70-76.
29. J. B. van Duuren, D. Wijte, B. Karge, V. A. dos Santos, Y. Yang, A. E. Mars and G. Eggink, *Biotechnol. Prog.*, 2012, **28**, 85-92.
30. S.-G. Bang and C. Y. Choi, *J. Ferment. Bioeng.*, 1995, **79**, 381-383.
31. D. R. Vardon, N. A. Rorrer, D. Salvachúa, A. E. Settle, C. W. Johnson, M. J. Menart, N. S. Cleveland, P. N. Ciesielski, K. X. Steirer, J. R. Dorgan and G. T. Beckham, *Green Chem.*, 2016, **18**, 3397-3413.
32. S. Mizuno, N. Yoshikawa, M. Seki, T. Mikawa and Y. Imada, *Appl. Microb. Biotechnol.*, 1988, **28**, 20-25.
33. T. Sonoki, K. Takahashi, H. Sugita, M. Hatamura, Y. Azuma, T. Sato, S. Suzuki, N. Kamimura and E. Masai, *ACS Sust. Chem. Eng.*, 2018, **6**, 1256-1264.
34. W. Wu, T. Dutta, A. M. Varman, A. Eudes, B. Manalansan, D. Loqué and S. Singh, *Scientific Rep.*, 2017, **7**, 8420.
35. J. G. Linger, D. R. Vardon, M. T. Guarnieri, E. M. Karp, G. B. Hunsinger, M. A. Franden, C. W. Johnson, G. Chupka, T. J. Strathmann, P. T. Pienkos and G. T. Beckham, *PNAS*, 2014, **111**, 12013-12018.
36. D. Salvachúa, E. M. Karp, C. T. Nimlos, D. R. Vardon and G. T. Beckham, *Green Chem.*, 2015, **17**, 4951-4967.
37. J. Ralph, *Phytochem. Rev.*, 2010, **9**, 65-83.
38. P. Calero, S. I. Jensen, K. Bojanovic, R. M. Lennen, A. Koza and A. T. Nielsen, *Biotechnol. Bioeng.*, 2018, **115**, 762-774.
39. M. M. Bagdasarian, E. Amann, R. Lurz, B. Ruckert and M. Bagdasarian, *Gene*, 1983, **26**, 273-282.
40. D. Salvachúa, R. Katahira, N. S. Cleveland, P. Khanna, M. G. Resch, B. A. Black, S. O. Purvine, E. M. Zink, A. Prieto, M. J. Martínez, A. T. Martínez, B. A. Simmons, J. M. Gladden and G. T. Beckham, *Green Chem.*, 2016, **18**, 6046-6062.
41. R. Katahira, A. Mittal, K. McKinney, X. Chen, M. P. Tucker, D. K. Johnson and G. T. Beckham, *ACS Sust. Chem. Eng.*, 2016, **4**, 1474-1486.
42. E. M. Karp, C. T. Nimlos, S. Deutch, D. Salvachúa, R. M. Cywar and G. T. Beckham, *Green Chem.*, 2016, **18**, 4750-4760.
43. M. S. Munson, E. M. Karp, C. T. Nimlos, M. Salit and G. T. Beckham, *ACS Sust. Chem. Eng.*, 2016, **4**, 7175-7185.
44. R. K. Jha, J. M. Bingen, C. W. Johnson, T. L. Kern, P. Khanna, D. S. Trettel, C. E. M. Strauss, G. T. Beckham and T. Dale, *Metab. Eng. Commun.*, 2018, **6**, 33-38.
45. P. I. Nikel, M. Chavarria, T. Fuhrer, U. Sauer and V. de Lorenzo, *J. Biol. Chem.*, 2015, **290**, 25920-25932.
46. N. Schweigert, A. J. Zehnder and R. I. Eggen, *Environ. Microbiol.*, 2001, **3**, 81-91.
47. L. R. Jarboe, L. A. Royce and P. Liu, *Frontiers Microb.*, 2013, **4**, 272.
48. L. N. Jayakody, C. W. Johnson, J. M. Whitham, R. J. Giannone, B. A. Black, N. S. Cleveland, D. M. Klingeman, W. E. Michener, J. L. Olstad, D. R. Vardon, R. C. Brown, S. D. Brown, R. L. Hettich, A. M. Guss and G. T. Beckham, *Energy Environm. Sci.*, 2018, **11**, 1625-1638.
49. Z. Tan, P. Khakbaz, Y. Chen, J. Lombardo, J. M. Yoon, J. V. Shanks, J. B. Klauda and L. R. Jarboe, *Metab. Eng.*, 2017, **44**, 1-12.
50. J. L. Ramos, E. Duque, M. T. Gallegos, P. Godoy, M. I. Ramos-González, A. Rojas, W. Teran and A. Segura, *Annu. Rev. Microbiol.*, 2002, **56**, 743-768.
51. N. S. Kruyer and P. Peralta-Yahya, *Curr. Opin. Biotechnol.*, 2017, **45**, 136-143.
52. L. Lin, Y. Cheng, Y. Pu, S. Sun, X. Li, M. Jin, E. A. Pierson, D. C. Gross, B. E. Dale, S. Y. Dai, A. J. Ragauskas and J. S. Yuan, *Green Chem.*, 2016, **18**, 5536-5547.
53. C. W. Johnson and G. T. Beckham, *Metab. Eng.*, 2015, **28**, 240-247.

TOC Image

